

Relaxation times of spin states of all ranks and orders of quadrupolar nuclei estimated from NMR *z*-spectra: Markov chain Monte Carlo analysis applied to ${}^7\text{Li}^+$ and ${}^{23}\text{Na}^+$ in stretched hydrogels

Philip W. Kuchel^{a,b,*}, Christoph Naumann^b, Max Puckeridge^b, Bogdan E. Chapman^b, David Szekely^c

^a Singapore Bioimaging Consortium, A*STAR, Singapore 138667, Singapore

^b School of Molecular Bioscience, University of Sydney, NSW 2006, Australia

^c Mark Cowley Lidwill Research Program in Cardiac Electrophysiology, Victor Chang Cardiac Research Institute, Darlinghurst, NSW 2010, Australia

ARTICLE INFO

Article history:

Received 6 May 2011

Revised 5 June 2011

Available online 14 June 2011

Keywords:

${}^7\text{Li}$ NMR

Aligned media in NMR

Markov chain Monte Carlo method

Parameter estimation

Residual quadrupolar coupling

Stretched gel

z-spectrum

ABSTRACT

The NMR *z*-spectra of ${}^7\text{Li}^+$ and ${}^{23}\text{Na}^+$ in stretched hydrogels contain five minima, or critical values, with a sharp “dagger” on the central dip. The mathematical representation of such *z*-spectra from spin-3/2 nuclei contains nine distinct (the total is 15 but there is redundancy of the \pm order-numbers) relaxation rate constants that are unique for each of the spin states, up to rank 3, order 3.

We present an approach to multiple-parameter-value estimation that exploits the high level of separability of the effects of each of the relaxation rate constants on the features of the *z*-spectrum. The Markov chain Monte Carlo (MCMC) method is computationally demanding but it yielded statistically robust estimates (low coefficients of variation) of the parameter values. We describe the implementation of the MCMC analysis (in the present context) and posit that it can obviate the need for using multiple-quantum filtered RF-pulse sequences to estimate all relaxation rate constants/times under experimentally favorable, but readily achievable, circumstances.

Crown Copyright © 2011 Published by Elsevier Inc. All rights reserved.

1. Introduction

The NMR ‘*z*-spectrum’ is a variant of the outcome of the saturation transfer experiment [1]: radio-frequency (RF) radiation is applied at frequency offsets across the whole NMR spectrum, and the total spectral integral is graphed as a function of the off-set frequency (e.g., [2]). For quadrupolar nuclei such as ${}^2\text{H}$ in HOD (spin-1; where D denotes deuterium) [2] and ${}^{23}\text{Na}^+$ (spin-3/2) [3] these nuclei in a hydrogel of gelatin or carrageenan, that is held stretched [4,5], show spectra with well-resolved residual quadrupolar couplings. The corresponding *z*-spectrum contains dips (minima) at frequencies that do not all correspond to the main Zeeman transitions of the simple pulse-and-acquire spectrum [2,3]. While the primary focus of the present paper is on a method of spectral analysis we also use the opportunity to present the *z*-spectrum of another spin-3/2 nucleus, ${}^7\text{Li}$. These data were used to estimate the values of relaxation rate constants of the various spin states of

both ${}^7\text{Li}^+$ and ${}^{23}\text{Na}^+$ in a way that appears to be novel (in the present context).

Whereas single quantum spectra of ${}^7\text{Li}$ and ${}^{23}\text{Na}$ contain three transitions in a 3:4:3 ratio, the *z*-spectra of ${}^7\text{Li}^+$ and ${}^{23}\text{Na}^+$ in stretched gelatin gel have five minima, or critical values, with a sharp “dagger” on the central dip. A mathematical representation of such *z*-spectra arises from the solution of the Liouville–von-Neumann equation that is modified by the addition of nuclear-magnetic relaxation [2,3,6,7]. Using the irreducible spherical tensor basis set [8,9], the form of the solution is a ratio of polynomials of high degree (degree 6 for spin-1 [2] and 12 for spin-3/2 [3]) in the off-set frequency of the partially saturating radiation; and the mathematical solution contains the nine relaxation rate constants (the total is 15 but there is redundancy of the \pm order-numbers) that are unique for each of the spin states up to rank 3, order 3 [3].

Conventionally, the values of the relaxation rate constants of a spin-3/2 nucleus are estimated by using various multiple-quantum-filter RF pulse sequences, to select particular spin states and hence their relaxation time courses (e.g., [3]). Here, we address the task of estimating all nine relaxation rate constants ($R_{1,0}, R_{1,1}, \dots, R_{3,3}$; where $R_{1,p}$ is the relaxation rate-constant for the tensor $T_{1,p}$) and the value of the residual quadruple coupling constant, ν_Q , from a family of 3–10 *z*-spectra. Optimism that this would be possible was based on the previous observation that

Abbreviations: FID, free induction decay; MCMC, Markov chain Monte Carlo; PGSE, pulsed field gradient spin-echo; RF, radio frequency.

* Corresponding author. Address: Singapore Bioimaging Consortium (SBIC), Agency for Science Technology and Research (A*STAR), 11 Biopolis Way, #02-02 Helios Building, Singapore 138667, Singapore. Fax: +65 8478 9957.

E-mail address: philip_kuchel@sbic.a-star.edu.sg (P.W. Kuchel).

the features of z -spectra of HOD in ^2H NMR [2], and $^{23}\text{Na}^+$ [3] are almost separately ascribable to each of the respective spin states, so that the values of the relaxation rate constants affect each feature in a distinct and almost unique way. This feature is akin to shimming the magnetic field of an NMR magnet with a set of “almost-orthogonal” magnetic field-gradient coils. E.g., we have shown that the central dagger in the z -spectrum is assignable to $T_{2,2}$ for $I = 1$ [2], and $T_{3,3}$ for $I = 3/2$ [3], so in simulating the latter data, increasing the value of $R_{3,3}$ decreases the depth of the dagger and nothing else in the z -spectrum; conversely, the values of no other relaxation rate constants affect the depth of the dagger [3].

In our previous fitting of z -spectra we used nonlinear regression to estimate the values of the relaxation rate constants of the spherical tensors, $T_{1,0}, T_{1,\pm 1}, \dots, T_{3,\pm 3}$ pertinent to $^{23}\text{Na}^+$ in a stretched gelatin gel. The fitting was only achieved in a practical time (several minutes) by iterating the regression process through small sets of the parameters (in *Mathematica* using the Levenberg, Marquardt, Morrison algorithm [10]) usually ‘floating’ three at a time. More elaborate algorithms have recently been described to handle multi-parameter problems; and they perform well with the fitting of certain types of model [11]. However, a much more direct approach that has become feasible with the greatly improved speed of laptop and desktop computers is the Markov chain Monte Carlo (MCMC) algorithm. The insights for this type of work are provided in the book by Jaynes [12] (completed posthumously by Bretthorst) and described recently in series of three lucid papers [13–15].

The outcome from the statistical analysis was a consistent set of estimates of the values of relaxation rate constants. Thus it may be experimentally valuable to discover that a particular spin-state with a special characteristic (e.g., large value) could be selected to interpret the physical environment of a group of spin-bearing ions or molecules. However, this aspect is not dealt with here as we concentrate on data-analysis: e.g., see other references for the use of long-lived states (that could first be revealed by the present method) for probing soft and hard material structures, by using pulsed field gradient spin-echo (PGSE) NMR spectroscopy [16,17].

2. Materials and methods

2.1. Theory of methods

The mathematical expression for a z -spectrum is derived by solving the equations of motion of the density operator (the caret denotes an operator) in Hilbert space as described previously [2,3]. This is given by the Liouville–von-Neumann equation [6–9],

$$\frac{d\hat{\rho}}{dt} = -i[\hat{H}, \hat{\rho}] \quad (1)$$

where $\hat{\rho}$ is the density operator, and \hat{H} is the Hamiltonian. When relaxation is included in the system of equations, Eq. (1) becomes:

$$\frac{d\hat{\rho}}{dt} = -i[\hat{H}, \hat{\rho}] - \hat{R}(\hat{\rho} - \hat{\rho}_{eq}) \quad (2)$$

where \hat{R} is the Redfield relaxation superoperator that acts on $\hat{\rho}$.

When the RF field is applied continuously for sufficiently long before acquiring the free induction decay (FID), the energy of the spin system reaches a steady state in which energy input from the RF field is balanced by losses via relaxation to the ‘lattice’. Thus, the derivative on the left-hand side of Eq. (2) becomes 0. By rearranging this equation, we obtain the expression for the steady-state density operator, $\hat{\rho}_{ss}$, which in the case of spin-3/2 nuclei is a 15×15 matrix [3].

The matrix was programmed in *Mathematica* [10] and was inverted and multiplied by the column vector $(0, -R_{1,0}, 0, 0, 0, 0, 0, 0, 0, 0, 0, 0, 0, 0, 0)^t$, where t denotes the transpose of this row vector, to give the z -spectrum. This spectrum was normalized to the

largest value for subsequent plotting and comparison with other such spectra. While an analytical expression can be obtained this way, as was done for the 8×8 element matrix for HDO in ^2H NMR, using the function *Inverse* [2,3] in *Mathematica* [10], its size and complexity for spin-3/2 made its evaluation best done numerically.

2.2. NMR methods

2.2.1. Spectrometer and data processing

^7Li and ^{23}Na NMR spectra were recorded at 155.51 and 105.4 MHz, respectively on a Bruker DRX 400 spectrometer (Bruker, Karlsruhe, Germany) with an Oxford Instruments (Oxford, UK) 9.4 T, vertical, wide-bore magnet.

Gaussian–Lorentzian deconvolution (Bruker, TopSpin 2) or manual integration were used, as relevant, to extract the relative areas of resonances in 1-dimensional (1D) spectra.

2.2.2. Pulse sequences

2.2.2.1. z -Spectra. For the z -spectra a ‘saturation transfer’ RF pulse sequence was used in which a period of low-power variable offset irradiation was followed by a phase-cycled $\pi/2$ pulse, then the FID was acquired. For $^7\text{Li}^+$ the selective partially saturating irradiation was achieved with a pulse of 10.0 s (12.0 s for 100% D_2O sample) duration (\sim five times the longest anticipated relaxation time) using a power-attenuation of ~ 69 –87 dB from a standard Bruker 300 W decoupling amplifier. The value of the attenuation factor was initially adjusted empirically to achieve full suppression of the signal in the un-stretched state of the sample. The acquisition time, aq , was 2 s; and the $\pi/2$ pulse duration, t_p , was 15.8 μs giving the Larmor frequency in the B_1 field, ν_1 , derived from the formula $\pi/2 = \gamma B_1 t_p = 2\pi\nu_1 t_p$, of 15822.8 rad s^{-1} . The irradiation frequencies were varied in small steps across the whole spectrum, from high to low frequency of the centre, beginning and ending where there was no apparent peak suppression. For the $^{23}\text{Na}^+$ z -spectra the procedure was the same but the RF-pulse conditions were as described in [3], with $t_p = 19.5 \mu\text{s}$ for the ι -carrageenan samples. Following standard 1D processing all spectra were deconvoluted. Each total integral was plotted as a fraction of that of the corresponding non-irradiated spectrum; i.e., it was normalized to the control spectrum.

2.2.2.2. Estimate of $R_{2,0}$. This estimate was made using the Jeener-Broekaert pulse sequence [18], as described in [3].

2.2.2.3. Estimates of $R_{1,0}$ and $R_{3,0}$. For these estimates a triple-quantum filter was used after a conventional inversion recovery pulse sequence, as described in [3]. The data were fitted by nonlinear regression analysis in *Mathematica* [10] to the function, $\text{Signal} = A_s e^{-\tau/T_{1s}} - A_f e^{-\tau/T_{1f}}$ where the pre-exponential A_s denote the amplitudes of the two components of the Signal (that is proportional to magnetization), and the subscripts, s and f , denote slow and fast, respectively.

2.2.2.4. Estimates of $R_{1,1}$, $R_{2,1}$ and $R_{3,1}$ of the respective one-quantum tensors. The relaxation times of the one-quantum irreducible spherical tensors were estimated from data acquired with a quadrupolar-echo RF pulse sequence as described in [3] with phase cycles as described by Halle and Furo [19], and Eliav and Navon [20].

Both sequences gave data that yielded, by nonlinear regression using *Mathematica* [10], different values for the relaxation rate constants for the centre peak and the two satellites.

2.2.2.5. Estimates of $R_{2,2}$ and $R_{3,2}$ of the, respective, double quantum tensors. The pulse sequence employed a double-quantum filter with a flip angle of 109.5° ($\cos 109.5^\circ = -1/3$). There was no refo-

cusing 180° pulse hence during the quadrupolar evolution time the frequency offset was set to that of the centre peak of the ${}^7\text{Li}^+$ triplet [3].

This pulse sequence yielded a magnetization time course that when fitted by a single exponential yielded an estimate of $R_{2,2}$ and $R_{3,2}$.

2.2.2.6. Estimates of $R_{3,3}$ of the triple-quantum tensor. The value of $R_{3,3}$ was estimated from data obtained with a triple-quantum-filter pulse sequence [3,9].

2.3. Markov chain Monte Carlo algorithm

Fig. 1 shows the logic-flow diagram for the MCMC algorithm; it involved the use of a random number generator (hence the name Monte Carlo) to incrementally increase or decrease the value of each element of a vector of parameter values, evaluate the function, and subtract the outcome from the previous value, thus yielding a 'residual'. If the summed square of residuals was less than that from the previous iteration, a secondary 'probability filter' caused the new vector to become the next or 'new' vector; if not the 'old' vector was used in the next iteration. The process was iterated a specified number of times, commonly 1000. It was possible to follow graphically the progress of the minimization of the sum of squares of the residuals, and to terminate the computation once a plateau in parameter values was evident. It was also possible to calculate the standard deviation of each parameter estimate using the accumulated chain of vectors (hence the term Markov chain) once the process had settled into a 'plateau' of function values, albeit with random fluctuations around a mean value.

2.4. Materials

2.4.1. Gels

For the ${}^7\text{Li}^+$ samples, gelatin (Gelita, Brisbane, QLD, grade 20N) solution (63% w/v in 1% D_2O , 99% H_2O ; or 100% D_2O) in its liquid state (usually at 60–80 °C) and containing 874 mM LiCl was drawn into a silicone rubber tube (for 10-mm NMR tubes Silastic® laboratory tubing from Dow Corning Corporation) that was sealed with a plug at one end, as previously described [2,3]. This tube was then inserted into a glass pipe (10-mm o.d.) so that when 'setting' occurred (at less than ~30 °C) the gel could be stretched with the silicone tube, and thus held extended by a thumb-screw that was positioned at the upper end of the outer glass pipe [2,3]. For the ${}^{23}\text{Na}^+$ samples in gelatin the procedure was the same except the gelatin solution (30–50% w/v in 100% D_2O) contained 154 mM NaCl. For the ${}^{23}\text{Na}^+$ samples in carrageenan, the ι -carrageenan C1138 was from Sigma–Aldrich (St. Louis, MO) and contained 154 mM NaCl.

3. Results

3.1. ${}^7\text{Li}^+$ spectra – H_2O

Fig. 2 shows a family of 10 ${}^7\text{Li}$ NMR (155.51 MHz) z -spectra acquired from LiCl in gelatin-gel constituted in H_2O and set in a silicone-rubber tube that was stretched to twice its original length and held firmly in this state. From the top spectrum (orange) to the bottom (red) the power was varied with an attenuation of the RF amplifier (~300 W) of 69–85 dB corresponding to power factors of ($\times 10^{-4}$) (3.5, 2.8, 2.2, 1.8, 1.4, 1.1, 0.89, 0.70, 0.56, 0.44). While it might be expected that the values of ν_1 used would be able to be calculated from the experimentally measured duration, t_p , of a $\pi/2$ pulse ($\pi/2 = \gamma B_1 t_p = 2\pi\nu_1 t_p$ and the attenuation factor is equal to $10^{-a/20}$ where a is the value of the attenuation in dB) it transpired that the most satisfactory fitting was achieved when these

values were 'floated' in the process; and the original calculated values of ν_1 were only used as starting values.

From Fig. 2 it was also seen that for the particular gelatin concentration used, and chosen extent of stretching, that the value of the residual quadrupolar coupling constant, ν_Q , was close to 10.8 Hz. Again, the best fits (lowest standard deviations) were obtained when this was only used as a starting value that was applicable to each z -spectrum and it was floated in the fitting procedure. Thus, the whole set of 10 z -spectra were fitted simultaneously with the initial values being set for ν_Q , 10 different values of ν_1 , and the nine relaxation rate constants giving a total of 20 parameter values to be estimated.

The initial estimates of the relaxation rate constants determined as described in the Methods section are given in Table 1. The values are all less by ~2 orders of magnitude than the corresponding values for ${}^{23}\text{Na}^+$ [3]; in other words the relaxation times of ${}^7\text{Li}^+$ were in the neighborhood of 1 s as opposed to 1–10 ms for ${}^{23}\text{Na}^+$. The values of the relaxation times as estimated by the MCMC method, and the various multiple-quantum filter experiments were similar but the estimates of the standard deviations were less with the new approach.

3.2. ${}^7\text{Li}^+$ relaxation times – D_2O

The values of the relaxation times of ${}^7\text{Li}^+$ were estimated from a gel constituted in D_2O ; these are the bottom numbers in each cell in the second column of Table 1. The basis for differences from those obtained in H_2O is of relevance to an explanation of the mechanism of relaxation of the various spin-states. However, it is readily apparent that the pairs of values were all very similar except for $T_{1,0}$ and $T_{3,0}$; on the other hand the relaxation times of all three of the second rank tensors were the same within the experimental error (overlap of mean values + or – two standard deviations) and the values of $T_{3,2}$ and $T_{3,3}$ were almost identical.

3.3. ${}^{23}\text{Na}^+$ spectra – previously reported data

Fig. 2 revealed systematic deviations of the lower three fitted curves from the experimental data but fitting to the central dagger was well captured by the algorithm. Based on the previous insights from 'visual' fitting of z -spectra [3] this was deemed to be important as the depth of the dagger closely reflects the value of $R_{3,3}$. On the other hand the value estimated by the previous approach was relatively low (last row of Table 1); and when this value was used in z -spectral simulations it was readily seen to be erroneous. In order to assess the veracity of this finding and to explore potential systematic errors in the MCMC approach we reanalyzed the data from [3].

Column 2 in Table 2 lists the previous [3] estimates of the relaxation times of the various tensors; and Column 3 shows the values that were estimated by fitting iteratively in groups of three parameters using conventional nonlinear least-squares regression [3]. The top number in each cell of Column 4 shows the final MCMC fit. The first entries in Columns 1–3, row 1 are all similar implying that the zero-order, longitudinal relaxation time was estimated "robustly" (similar values) by all three approaches and notably by the MCMC method. The three estimates each of $T_{2,0}$, and $T_{2,1}$ were all similar and yet in the previous regression analysis [3] the estimate of $T_{3,2}$ was larger by a factor of two while with the MCMC method it was less. The most notable difference between the estimates made by using the multiple-quantum filter method and nonlinear regression analysis of the z -spectra was the estimate of $T_{3,3}$. Since the value of $T_{3,3}$ is the almost exclusive determinant of the depth of the central dagger in the z -spectrum it was concluded that the multiple-quantum filter method was in error; the larger estimate was reconfirmed in the MCMC analysis, which returned

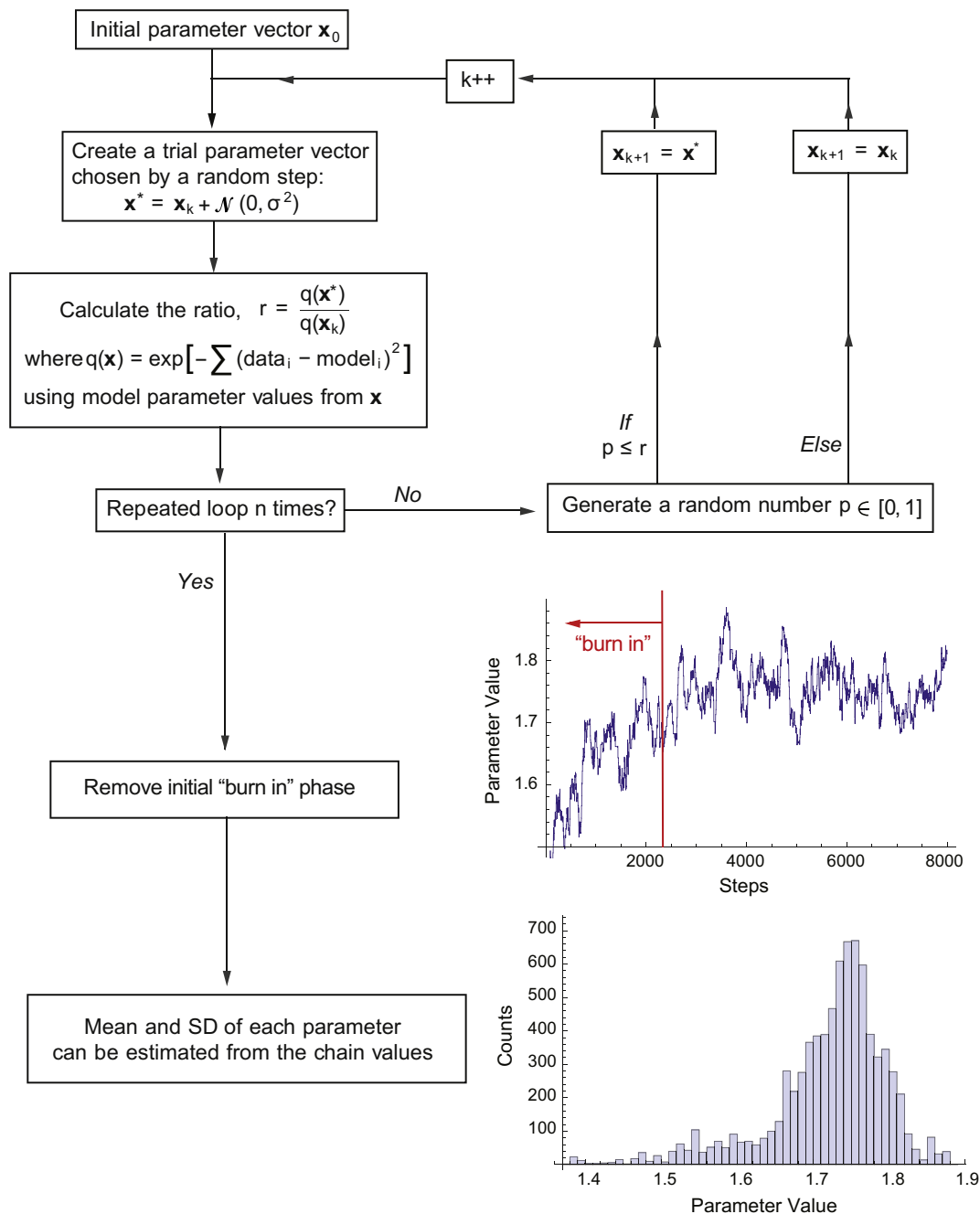


Fig. 1. Flow diagram of the MCMC algorithm. The input vector of initial estimates of the parameter values is denoted \mathbf{x}_0 . The random number chosen from a normal distribution is denoted $\mathcal{N}(0, \sigma^2)$ where σ^2 is the variance of a gaussian distribution, centred on 0; in *Mathematica* [10] such random numbers are based on Rule 30 of a 3-unit cellular automaton. The value of r is computed as indicated in the third box on the left and its value is tested against a 'probability factor' whose value is chosen empirically so that $\sim 20\%$ of the 'new' values of the vector \mathbf{x} are used in the next iteration of the loop. An initial phase of the total number of iterations is called the 'burn in' phase and the values of \mathbf{x} before this phase are discarded, while the remainder are used to construct a histogram and to calculate the standard deviation of each of the elements of \mathbf{x} .

a value close to (12.4 ms versus 15.0 ms) that from the nonlinear regression analysis.

3.4. $^{23}\text{Na}^+$ spectra-from ι -carrageenan gel

Based on work with carrageenan gels with their high concentration of charged sulfate groups [21] but low overall gel concentration (as compared to gelatin gels) it was expected that the relaxation times of the various tensors would differ from those estimated from gelatin gels. Three $^{23}\text{Na}^+$ NMR z-spectra obtained from ι -carrageenan gels are shown in Fig. 3. MCMC analysis was performed on this small set and the very close fit of the z-spectrum

function is evident, with special note of the central dagger. The estimate of $T_{3,3}$ was the largest of all the relaxation times, as was the case for gelatin. Indeed it was higher than the value for gelatin, as were $T_{2,1}$, $T_{2,2}$, $T_{3,1}$, and $T_{3,2}$. The only markedly lower value than for gelatin was $T_{1,1}$.

4. Discussion

4.1. MCMC performance

On searching for a global minimum when applying the MCMC algorithm to z-spectral data it was essential to have initial

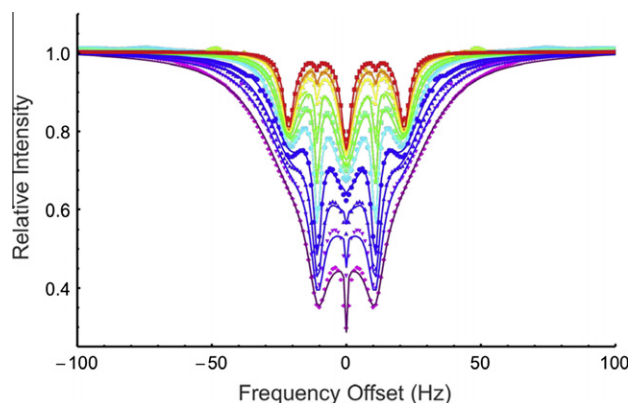


Fig. 2. ^7Li NMR (155.51 MHz) z-spectra (steady-state irradiation envelopes; normalized to the control spectrum) of $^7\text{Li}^+$ in stretched (by a factor of ~ 2) gelatin gel. The family of 10 z-spectra were acquired with the partially saturating RF field delivered at the indicated offset frequencies and of the following power-attenuation factors (see Section 2) (in dB), respectively: red 87; maroon 85; purple 83; violet 81; blue 79; aquamarine 77; light green 75; dark green 73; yellow 71; and orange 69. A saturation transfer RF sequence was used with an RF flip angle of 90° invoked with a pulse of $15.6 \mu\text{s}$, a repetition time of 12.0 s, and with 8 transients per spectrum. A line-broadening factor of 0.5 Hz was applied prior to Fourier transformation of the FID. The sample was thermostatted in the NMR probe at 15°C . (For interpretation of the references to colour in this figure legend, the reader is referred to the web version of this article.)

estimates that were within and order of magnitude of the ‘true’ value. For this reason preliminary multiple-quantum filtered-based estimates were valuable. Then a series of runs were performed with a number of iterations around 1000 and a choice of increment values that were $\sim 1/100$ to $1/1000$ the initial estimate of each parameter value. Finally having observed that the parameter estimates each approached a plateau value the set of estimates was concluded to be at the local minimum of the multi-dimensional parameter space. Re-running the algorithm using these values as starting values led to estimates of standard deviations obtained from the respective distribution of values around the mean that approached zero. This is clearly incorrect: so to obtain an estimate of the standard deviation of parameter estimates it was necessary

to increase the value of the decrement to $\sim 1/100$ th of the mean value. By doing this, random variations in the set of parameter values causes all values to vary significantly and thus ‘map out’ a large neighborhood of the local minimum over the iteration time course; thus over the fitting trajectories all parameters take on a distribution of values from which a standard deviation can be estimated. This process is tantamount to a ‘sensitivity analysis’ that is used in studying the dependence of the output of a mathematical model on the values of its parameters, say of a metabolic system whose kinetics are described by an array of nonlinear differential equations [22].

The MCMC method of regression analysis led to objective fitting of families of z-spectra. Of particular note was the extent to which the fitting readily captured the details of the central dagger and hence allowed the estimate of $T_{3,3}$. This value was less reliably estimated by using the approach with multiple-quantum filtered spectra.

4.2. Variations between types of hydrogel

The estimated values of the relaxation times of $^{23}\text{Na}^+$ in ι -carrageenan gels were in most cases higher than for gelatin. ι -Carrageenan is a poly-sulfated carbohydrate polymer so it is likely that the sulfate groups bind and thus sequester paramagnetic ions; this decreases the rate of relaxation of various spin states that would otherwise interact with paramagnetic ions. On the other hand the value of $T_{2,1}$, which is equivalent to the conventional T_2 , was shorter. This can be ascribed to the rapid exchange of the $^{23}\text{Na}^+$ ions on and off the sulfate groups [21]. A detailed analysis of the mechanistic basis of the different relaxation times, however, was not the focus of the present work and will be dealt with elsewhere.

4.3. Systematic deviations in parameter estimates

The differences in mean values of relaxation rate constants estimated by the standard approach and the MCMC method (Tables 1 and 2) begs an explanation. Possible errors in the theory, or their application in computer programs, of the multiple-quantum filter

Table 1
Relaxation times of the nine spin states of different rank and order that corresponded to the irreducible spherical tensors of $^7\text{Li}^+$ in stretched gelatin gel in $\text{H}_2\text{O}^{\text{a}}$ and $\text{D}_2\text{O}^{\text{b}}$. The subscripts refer to the corresponding tensor. The relaxation times with a right-hand zero subscript are longitudinal relaxation times; those with 1 in this position are the ‘conventional’ R_2 times ($1/T_2$); while those with 2 or 3 in this position describe transverse relaxation of two- and three-quantum states, respectively.

Relaxation times	Experimental value (1/R; s)	Experiment type and fitting function	MCMC-fitted value (1/R; s)
$T_{1,0} = 1/R_{1,0}$	$3.03 \pm 0.04^{\text{a}}$ $3.57 \pm 0.12^{\text{b}}$	Biexponential fit for $T_{3,0}$, and $T_{1,0}$	$8.6 \pm <0.01^{\text{c}}$
$T_{1,1} = 1/R_{1,1}$	0.47 ± 0.02 0.30 ± 0.02	Single exponential fit; same value as $T_{3,1}$	0.80
$T_{2,0} = 1/R_{2,0}$	1.02 ± 0.08 1.20 ± 0.09	Jeener–Broekart and single exponential fit	4.6
$T_{2,1} = 1/R_{2,1}$	0.62 ± 0.04 0.61 ± 0.05	Single exponential fit	0.43
$T_{2,2} = 1/R_{2,2}$	0.26 ± 0.03	^d Average of values for three peaks; could not fit a biexponential; should give two values, one each for $T_{2,2}$ and $T_{3,2}$	0.11
$T_{3,0} = 1/R_{3,0}$	0.25 ± 0.04 0.59 ± 0.06 0.86 ± 0.07	Biexponential fit gives $T_{3,0}$, and $T_{1,0}$	3.0
$T_{3,1} = 1/R_{3,1}$	0.47 ± 0.02 0.30 ± 0.02	Single exponential fit; same value as $T_{1,1}$	0.56
$T_{3,2} = 1/R_{3,2}$	0.26 ± 0.03 0.25 ± 0.04	^d See above	0.11
$T_{3,3} = 1/R_{3,3}$	0.21 ± 0.03 0.20 ± 0.02	Single exponential fit	0.18

^a The upper number in each cell in this column is the value estimated with $^7\text{LiCl}$ and gelatin dissolved in H_2O .

^b The lower number in each cell in this column is the value estimated with $^7\text{LiCl}$ and gelatin dissolved in D_2O .

^c All standard deviations were less than 0.001.

Table 2

Comparison of previous estimates reported in [3] (Columns 1–3), of the nine relaxation times that correspond to the irreducible spherical tensors of $^{23}\text{Na}^+$ in stretched gelatin gel in D_2O , with the same data subjected to MCMC analysis (Column 4). The parameter names are the same as in Tables 1 and 2; and the new values estimated for $^{23}\text{Na}^+$ in stretched ι -carrageenan gel (Column 5).

Column 1 Relaxation parameter	Column 2 Previous [1] experimental estimate (1/R; ms) (gelatin)	Column 3 Previous [1] piecewise regression estimate (1/R; ms) (gelatin)	Column 4 MCMC-fitted estimate (1/R; ms) (gelatin)	Column 5 MCMC-fitted estimate (1/R; ms) (carrageenan)
$T_{1,0} = 1/R_{1,0}$	11.2 ± 1.2 11.8 ± 1.0	10.0	12.4 ± 0.001^a 10.6 ± 0.02^b	$7.7 \pm <0.001^c$
$T_{1,1} = 1/R_{1,1}$	8.0 ± 0.3	7.0	10.5 ± 0.2 9.4 ± 0.07	2.3
$T_{2,0} = 1/R_{2,0}$	5.3 ± 1.0 3.3 ± 0.11	5.0	5.6 ± 0.02 4.9 ± 0.02	4.2
$T_{2,1} = 1/R_{2,1}$	1.9 ± 0.1	3.5	2.05 ± 0.01 2.0 ± 0.004	8.5
$T_{2,2} = 1/R_{2,2}$	2.1 ± 0.06	3.0	7.1 ± 0.06 6.9 ± 0.02	11.9
$T_{3,0} = 1/R_{3,0}$	4.4 ± 0.5	4.0	7.7 ± 0.04 6.4 ± 0.02	4.8
$T_{3,1} = 1/R_{3,1}$	8.3 ± 0.3	2.0	7.3 ± 0.05 6.3 ± 0.01	11.9
$T_{3,2} = 1/R_{3,2}$	2.1 ± 0.06	5.0	1.1 ± 0.003 1.2 ± 0.01	7.3
$T_{3,3} = 1/R_{3,3}$	7.7 ± 0.1	15.0	12.4 ± 0.1 8.3 ± 0.04	19.1

^a The upper number in each cell in this column is the final estimate after plateaux of trajectories of values in the 4000 iterations of the MCMC analysis with increments on the $R_{i,p}$ values of $R_{i,p}/200$, on the $v_{1,i}$ values of $v_{1,i}/500$, and on v_Q of $v_Q/1000$.

^b The lower number in each cell in this column is the estimate after 4000 iterations of the MCMC analysis with increments on the $R_{i,p}$ values of $R_{i,p}/500$, on the $v_{1,i}$ values of $v_{1,i}/500$, and on v_Q of $v_Q/1000$. Plateaux were not achieved in the trajectories, for the three values $v_{1,i}$, $i = 1, \dots, 3$, $R_{3,2}$, and $R_{3,3}$.

^c In this column the data set (shown in Fig. 3) consisted of three z-spectra with different $v_{1,i}$ values, with increments on the $R_{i,p}$ values of $R_{i,p}/200$, on the $v_{1,i}$ values of $v_{1,i}/200$, and on v_Q of $v_Q/500$. The standard deviations were all less than 0.001.

approach, or the Liouvillian theory used here, appear to be unlikely as several authors have independently performed simulations using their own algorithms. So the most likely explanation is found in the experimental set up. Obtaining hydrogel samples that give reproducible NMR spectral responses demands careful attention to the source of the gel and its batch number. This potential variation was eliminated in the present work by using replicate measurements on the same batch of gel that gave results that were the same within experimental error. This leaves two other sources of discrepancy, namely the calibration of RF pulse durations with nutation angle (or magnetization), and avoidance of the effect of ‘progressive saturation of magnetization’ when averaging FIDs. In the present work the former was assiduously addressed. However, the latter effect is the likely explanation for the differences in parameter estimates that are shown especially in Table 1.

With the conventional inversion recovery RF pulse sequence, that is used to estimate the value of T_1 , the failure to record the signal after a sufficiently long delay means that the signal is mistakenly taken to have plateaued before the spin system has fully relaxed. Therefore, when fitting a rising exponential function to the data the estimated relaxation rate constant is larger (‘faster’) than the ‘true’ value. In other words the method underestimates the value of T_1 .

When z-spectra are generated, RF irradiation is applied to the sample for sufficiently long so that a true steady-state is set up between the energy input from the RF field and that dissipated by the spin-system to the surroundings (lattice). It is conventional practice when performing these experiments, and in fact for the measurement of all relaxation times, to use inter-transient delays of at least five times the longest relaxation time (usually T_1). For z-spectra the theory embodied by Eq. (2) assumes that the time derivative of the density operator is zero, but if the system has not reached a steady state before each FID is recorded then the power delivered will be less than is calculated using the arguments given in Section 2.2.2.1. The fact that it was not possible to obtain ‘reasonable’ MCMC fits to the z-spectra in the present work, using the calculated v_1 values (but we used these as starting values in the

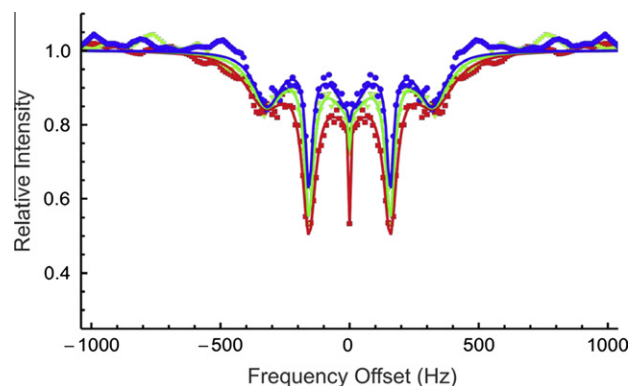


Fig. 3. ^{23}Na NMR (105.4 MHz) z-spectra from $^{23}\text{Na}^+$ in stretched ι -carrageenan gel. The three z-spectra were acquired with the partially saturating RF field delivered at the indicated offset frequencies and using the following power-attenuation factors (see Section 2) (in dB), respectively: red 55; green 53; blue 51. A saturation transfer RF pulse sequence was used with an RF flip angle of 90° invoked with a pulse of $19.5 \mu\text{s}$, a repetition time of 10.0 s, and with 8 transients per spectrum. A line-broadening factor of 0.5 Hz was applied prior to Fourier transformation of the FID. The sample was thermostatted in the NMR probe at 15°C . (For interpretation of the references to colour in this figure legend, the reader is referred to the web version of this article.)

MCMC fitting), is consistent with the system not having been in a ‘true’ steady state.

The intellectual challenge is to ascertain if this situation leads to an under- or an over-estimate of the various relaxation times. We posit that at least for $T_{1,0}$ ($1/R_{1,0}$) it is over estimated, in contrast to the situation with the simple inversion recovery method. If a steady state of RF-input energy is not attained, then the effective value of v_1 will be less than calculated (Section 2.2.2.1). In Figs. 2 and 3 (and in the top right, inset of Fig. 1 in [3]) it is seen that increasing the value of v_1 increases the overall depth of the z-spectrum; in other words the various features (minima) are ‘deepened’ as v_1 is increased. If the effective value of v_1 is less than calculated then the z-spectrum will be less deep than expected. On the other hand,

in the top left panel of Fig. 2 in [3], it is seen that for a given value of ν_1 , increasing the value of $T_{1,0}$ ($1/R_{1,0}$) deepens the z-spectrum. Thus in a situation in which a true steady state does not exist between the energy input via the partially saturating RF field and the dissipation by the spin-system to the surroundings, the experimental z-spectrum will only be able to be realistically simulated (by using the theory), if a larger value (than is the ‘true’ one) is chosen for $T_{1,0}$ ($1/R_{1,0}$). In other words, in a simulation, the lower effective ν_1 is compensated for by choosing (fitting) a larger value of $T_{1,0}$.

Overall this means that a common error in the implementation of the z-spectrum experiment, namely failing to apply the partially saturating RF irradiation for sufficiently long, will lead to an overestimate of $T_{1,0}$. The situation regarding the other relaxation times is more complex to understand at an intuitive level, and this will require future theoretical and experimental studies.

5. Conclusions

In conclusion, the MCMC approach to multiple parameter-value estimation performed well with sets of z-spectra from both ${}^7\text{Li}^+$ and ${}^{23}\text{Na}^+$. These spin-3/2 nuclei with relaxation times in very different time scales (different by a factor of ~ 100) nevertheless yielded z-spectra that readily revealed a global minimum in multi-dimensional ($10 +$ the number of z-spectra) parameter space. The apparent separability of the effects of the parameter values on the features of the z-spectra meant that the MCMC algorithm performed well in spite of the very large dimensionality of the parameter space. This property of z-spectra makes them a useful form of spectral analysis for probing properties of materials than can be inferred from the different relaxation times of tensors of different ranks and orders; and MCMC analysis provides a systematic way of estimating all relaxation times including those that report on particular physico-chemical features of a sample (e.g., [23]) provided the caveats alluded to in Section 4.3 are heeded.

Acknowledgments

The work was funded by a Discovery Project grant from the Australian Research Council to PWK and Professor Jamie Vandenberg, who is also thanked for valuable discussions. MP has an

Australian Postgraduate Award. We thank Gelita, Brisbane, QLD, for the gift of gelatin. Dr Uzi Eliav is thanked for valuable discussions on the mathematical forms of z-spectra. Dr David Philp is thanked for discussions on data analysis using the MCMC method and for developing Ptolemy IV that was used in the derivation of the mathematical expression for z-spectra. The *Mathematica* program containing the MCMC algorithm and a representative set of ${}^7\text{Li}^+$ z-spectral integrals in a Microsoft Excel file that is read in by the program, are available from PWK.

References

- [1] J. Grad, R.G. Bryant, J. Magn. Reson. 90 (1990) 1–8.
- [2] U. Eliav, C. Naumann, G. Navon, P.W. Kuchel, J. Magn. Reson. 198 (2009) 197–203.
- [3] B.E. Chapman, C. Naumann, D. Philp, U. Eliav, G. Navon, P.W. Kuchel, J. Magn. Reson. 205 (2010) 260–268.
- [4] P.W. Kuchel, B.E. Chapman, N. Müeller, W.A. Bubba, D.J. Philp, A.M. Torres, J. Magn. Reson. 180 (2006) 256–265.
- [5] G. Kummerlöwe, F. Halbach, B. Laufer, B. Luy, Open Spectrosc. J. 2 (2008) 29–33.
- [6] P.J. Hore, J.A. Jones, S. Wimperis, NMR: The Toolkit, Oxford University Press, Oxford, 2000.
- [7] M.H. Levitt, Spin Dynamics, second ed., John Wiley & Sons, Chichester, UK, 2008.
- [8] N. Müller, G. Bodenhausen, R.R. Ernst, J. Magn. Reson. 75 (1987) 297–334.
- [9] C.W. Chung, S. Wimperis, Mol. Phys. 76 (1992) 47–81.
- [10] S. Wolfram, The *Mathematica* Book, Version 8.0.1.0. Wolfram Media Inc., Champaign, IL, 2011.
- [11] D. Szekeley, J.I. Vandenberg, S. Dokos, A.P. Hill, Med. Biol. Eng. Comput. 49 (2011) 289–296.
- [12] E.T. Jaynes, Probability Theory: The Logic of Science, Cambridge University Press, Cambridge, UK, 2003 (5th printing, 2009).
- [13] G.L. Bretthorst, W.C. Hutton, J. R. Barbow, J.J.H. Ackermann, Concepts Magn. Reson. A 27A (2005) 55–63.
- [14] G.L. Bretthorst, W.C. Hutton, J. R. Barbow, J.J.H. Ackermann, Concepts Magn. Reson. A 27A (2005) 64–72.
- [15] G.L. Bretthorst, Concepts Magn. Reson. A 27A (2005) 63–73.
- [16] S. Cavadini, P.R. Vasos, Concepts Magn. Reson. A 32A (2008) 68–78.
- [17] N.N. Yadav, A.M. Torres, W.S. Price, J. Magn. Reson. 204 (2010) 346–348.
- [18] R.J. Kemp-Harper, Development of Multi-Pulse NMR Methods for Investigation of Sodium Ions In Vivo. DPhil Thesis, Exeter College, Oxford University, UK, 1997 (Supervisors: S. Wimperis, P. Styles).
- [19] B. Halle, I. Furo, J. Magn. Reson. 98 (1992) 388–407.
- [20] U. Eliav, G. Navon, J. Magn. Reson. A 115 (1995) 241–253.
- [21] C. Naumann, P.W. Kuchel, Polym. Chem. 1 (2010) 1109–1116.
- [22] P.J. Mulquiney, P.W. Kuchel, Modelling Metabolism with *Mathematica*, CRC Press, Boca Raton, FL, 2003.
- [23] J. Kowalewski, L. Mäler, Nuclear Spin Relaxation in Liquids: Theory Experiments and Applications, Taylor and Francis, NY, 2006.